

Prediction of Thermal Emission and Exchange Among Neighboring Wavelength-Sized Spheres

Daniel W. Mackowski

Department of Mechanical Engineering,
Auburn University,
Auburn, AL 36849
e-mail: mackodw@auburn.edu

Michael I. Mishchenko

NASA Goddard Institute for Space Studies,
2880 Broadway,
New York, NY 10025

An analysis of radiative emission and radiative exchange among an ensemble of closely spaced, wavelength-sized spheres, in which each sphere in the ensemble is at a distinct and uniform temperature, is presented. We show that the rate of spectral emission from a specific sphere in the ensemble and the rate at which emission is exchanged between a pair of spheres can be deduced from the application of reciprocity and energy conservation principles to the solution of Maxwell's time harmonic wave equations for a sphere ensemble that is exposed to a plane wave incident field of wavelength λ . We show that in the limit of $d/\lambda \rightarrow 0$, the emissive exchange between a pair of spheres becomes inversely proportional to the gap thickness d . We also show that when the spheres are in the mutual far-field zones of each other, the emissive exchange between the spheres can be well approximated by geometric configuration factors, with an effective area correction to account for finite wavelength effects. [DOI: 10.1115/1.2957596]

Keywords: nanoscale heat transfer, electromagnetic scattering, spheres, radiative heat transfer

1 Introduction

The objective of this article is to develop an exact prediction of the thermal radiation heat transfer exchanged between small neighboring spheres. By “small” and “neighboring,” we are referring to spheres that have radii comparable to the visible and IR wavelengths of thermal radiation and that are located in the mutual near-field zones that characterize the thermal radiation. Our motivation in addressing this topic is, to a large part, simply one of academic interest and academic continuity: a large body of work has been assembled on the plane wave scattering properties of multiple sphere systems, and we wish to extend this work to delineate the intersphere energy transport processes. The topic, however, is certainly relevant to a variety of situations in the emerging fields of nano- and microscale transport phenomena. In particular, a detailed understanding of the microscopic-level energy transport process in deposits of nanometer- and micrometer-sized particles—which is necessary for the prediction of the optical and photonic properties of the deposits—will require an improved ability to predict energy transfer on the individual-particle scale.

The wavelength-sized length scales of our system will certainly preclude the application of a macroscopic-level radiant exchange analysis. Our approach to the problem will be to employ solutions to Maxwell's macroscopic wave equations for multiple spheres to characterize the electromagnetic energy flow from and among the spheres that results from thermal emission. Beginning with the pioneering work of Brunning and Lo, a great deal of analytical and computational resources have been developed to determine the absorption and scattering properties of multiple sphere systems [1–3]. Even though the solution can identify the absorption cross section of individual spheres in the ensemble—for both fixed and random orientations relative to the incident wave—the

prediction of thermal emission from individual spheres or the rate of intersphere energy transfer has not been addressed in these works.

An analysis of thermal emission from a micrometer-sized homogeneous and isothermal sphere was first examined by Kattawar and Eisner [4], who employed the Rytov model in which thermal emission is modeled as fluctuating electric polarization [5]. Their model provided a detailed confirmation of Kirchhoff's law in that the spectral emission cross section of the sphere was shown to be equal to the absorption cross section as predicted by the Lorenz–Mie theory. The exchange of thermal radiation between a small spherical particle, modeled as an electric dipole, and a plane surface was formulated by Mulet et al., and their analysis shows that the coupling of evanescent waves can lead to a significant increase in heat transfer when the sphere is in the near-field zone of the surface [6]. More recently, Narayanaswamy et al. applied the Rytov model to predict the thermal emission exchange between a pair of arbitrarily sized spheres [7]. This analysis enabled, for the first time, an exact determination of intersphere thermal energy transfer for pairs of spheres that are separated by subwavelength distances. However, they report that their solution develops convergence problems as the two spheres approach contact. In addition, it is not obvious from their work how their solution corresponds or connects to the existing understanding of absorption and scattering by sphere clusters.

A key goal in the present work is to develop a general formulation for thermal emission by, and exchange among, the individual spheres in a multiple sphere ensemble. To this end, we will not model emission explicitly via the Rytov formulation. Rather, we will begin with the plane wave scattering formulation for the sphere cluster and develop, via equilibrium and reciprocity arguments, the formulas which predict the emissive flow of energy among the spheres.

2 Formulation

2.1 Definition of the Emission Cross Section. The model we use in our analysis is illustrated in Fig. 1, which consists of a

Contributed by the Heat Transfer Division of ASME for publication in the JOURNAL OF HEAT TRANSFER. Manuscript received August 22, 2007; final manuscript received January 11, 2008; published online September 3, 2008. Review conducted by Walter W. Yuen.

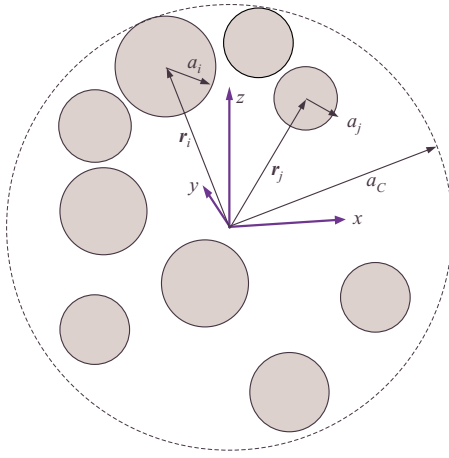


Fig. 1 Ensemble configuration

system of N_S spheres denoted by $i=1, 2, \dots, N_S$. Each sphere is characterized by a position \mathbf{r}_i (relative to a common coordinate origin), a radius a_i , and a complex refractive index $\mathbf{m}_i = n_i + ik_i$ (which, in general, will be dependent on the wavelength of radiation). The system is surrounded by a large (and black) environment.

In the most general case, we will take each of the spheres to be maintained, via some unseen means, at a distinct yet uniform temperature of T_i , and likewise the environment is at a temperature of T_e . One consequence of the isothermal-sphere model is that the spheres are assumed to be separated from their neighbors to avoid the existence of a discontinuous temperature jump at a contact point. We wish to predict the monochromatic power (or, synonymously, thermal radiative heat transfer) emitted from and absorbed by each of the spheres and to also identify the detailed exchange of thermal radiation among the spheres (i.e., the fraction of the power emitted by i , which is absorbed by j).

Our analytical route to this goal will begin with the observation that the net rate of monochromatic thermal emission from a sphere must be proportional to the spectral blackbody intensity $I_{b,\lambda}(T_i)$ evaluated at the sphere temperature. It is therefore consistent to state that

$$q_{i,\lambda} d\lambda = 4\pi C_{\text{emis},i} I_{b,\lambda}(T_i) d\lambda \quad (1)$$

where $q_{i,\lambda}$ denotes the heat transfer contained within the wavelength interval $d\lambda$ and $C_{\text{emis},i}$ denotes a monochromatic emission cross section for sphere i (units of area). This cross section would depend not only on the properties of sphere i , but also on the optical properties and positions of all the neighboring spheres in the system. However, since we are considering only spontaneous emission, the cross section will not be a function of the radiative field incident on the sphere; in particular, it would be decoupled from the temperatures of the surrounding spheres and the environment. Second, a detailed and identifiable accounting must exist for the radiation emitted from sphere i ; a fraction of the radiation will be absorbed by sphere 1, a different fraction by 2, etc., and whatever is not absorbed by the spheres will be absorbed by the environment. Therefore, we can postulate the property of an exchange cross section $C_{\text{emis},i-j}$ so that $4\pi C_{\text{emis},i-j} I_{b,\lambda}(T_i) d\lambda$ is the power emitted from i and absorbed by j . Since all the radiation from i must end up somewhere, then

$$C_{\text{emis},i} = C_{\text{emis},i-e} + \sum_{\substack{j=1 \\ j \neq i}}^{N_S} C_{\text{emis},i-j} \quad (2)$$

in which subscript e denotes the environment. Note that by excluding $j=i$ from the sum, we imply that self-absorption is included into the definition of $C_{\text{emis},i}$ in Eq. (1). Third, thermody-

namical considerations will prohibit the net exchange of heat between two sites i and j that are at the same temperature. This establishes the reciprocity condition of

$$C_{\text{emis},i-j} = C_{\text{emis},j-i} \quad (3)$$

For any particle, it is known that the absorption of thermal emission from the isothermal environment by the particle is equivalent to the absorption of unpolarized plane wave radiation having the same blackbody intensity and averaged over all incident directions [8]. This concept can also be extended to each subunit within the particle; for the problem at hand, the absorption by sphere i of thermal emission from the environment—which will be $4\pi C_{\text{emis},i-e} I_{b,\lambda}(T_e) d\lambda$ —will be equal to the random-incidence plane wave absorption by the sphere. It follows that

$$C_{\text{emis},i-e} = \langle C_{\text{abs},i} \rangle \quad (4)$$

where $\langle C_{\text{abs},i} \rangle$ denotes the orientation-averaged absorption cross section of sphere i .

A well-developed formulation exists for the prediction of the absorption cross section of an individual sphere in an ensemble—in both fixed and random orientation—and this formulation will be reviewed in the following section. What has not been performed and what is presented here is a decomposition of the absorption cross section into components which account for the intersphere energy transfers implied in Eq. (2). In particular, we intend to identify the exchange cross sections so that

$$\langle C_{\text{abs},i} \rangle = C_{\text{emis},i-e} = C_{\text{emis},i} - \sum_{\substack{j=1 \\ j \neq i}}^{N_S} C_{\text{emis},i-j} \quad (5)$$

2.2 Multiple Sphere Scattering Formulation

2.2.1 Superposition Model and the Interaction Equations. Only those aspects of the multiple sphere scattering formulation which are directly relevant to the problem at hand will be presented here; the reader is referred to Refs. 2 and 9 for details. In the solution, the field external to the spheres is constructed from a superposition of the incident field and fields scattered from each sphere in the ensemble,

$$\mathbf{E}_{\text{ext}} = \mathbf{E}_{\text{inc}} + \sum_{i=1}^{N_S} \mathbf{E}_{\text{sca},i} \quad (6)$$

For each sphere, the incident and scattered fields can be represented by an expansion of vector spherical harmonics (VSH), centered about the origin of the sphere,

$$\mathbf{E}_{\text{inc},i} = \sum_{n=1}^{L_i} \sum_{m=-n}^n \sum_{p=1}^2 p_{mnp}^i \mathbf{N}_{mnp}^{(1)}(\mathbf{r} - \mathbf{r}_i) \quad (7)$$

$$\mathbf{E}_{\text{sca},i} = \sum_{n=1}^{L_i} \sum_{m=-n}^n \sum_{p=1}^2 a_{mnp}^i \mathbf{N}_{mnp}^{(3)}(\mathbf{r} - \mathbf{r}_i) \quad (8)$$

In the above, \mathbf{N}_{mnp} denotes the VSH of either type 1 (regular, based on the spherical Bessel function $j_n(kr)$) or 3 (outgoing, based on the spherical Hankel function $h_n = j_n + iy_n$) and of order n , degree m , and mode $p=1$ (TM) or 2 (TE). The order truncation limit L_i in Eq. (8) is chosen to provide an acceptable precision in the calculated scattering properties of the cluster; L_i can typically be set using the Lorenz–Mie criterion, although in certain cases the neighboring spheres can have a significant effect on the convergence of Eq. (8) [9].

The incident field coefficients p^i will depend on the propagation direction and polarization state of the incident field (which typically is a plane wave) and the relative position of origin i , whereas the scattering coefficients a^i are initially unknown and are sought from the analysis. A relationship between the incident and scattered field coefficients can be obtained via a generalized applica-

tion of the Lorenz–Mie theory for a sphere, in which the exciting field for a particular sphere includes the incident field as well as the fields scattered from all other spheres. This analysis leads to a set of interaction equations, the solution of which provides a linear relationship of the form

$$a_{mnp}^i = \sum_{j=1}^{N_S} \sum_{l=1}^{L_j} \sum_{k=-l}^l \sum_{q=1}^2 T_{mnpklq}^{i-j} p_{klq}^j \quad (9)$$

in which the sphere-sphere T^{i-j} matrix is given by the solution to the following matrix interaction equations:

$$\frac{1}{\bar{a}_{np}^i} T_{mnpklq}^{i-j} - \sum_{j'=1}^{N_S} \sum_{l'=1}^{L_{j'}} \sum_{k'=-l'}^{l'} \sum_{q'=1}^2 H_{mnpk'l'q'}^{i-j'} T_{k'l'q'klq}^{j'-j} = \delta_{ij} \delta_{mk} \delta_{nl} \delta_{pq} \quad (10)$$

$j' \neq i$

In the above, δ_{ij} is the Kronecker delta function, \bar{a}_{np}^i denotes the Lorenz–Mie coefficients of the sphere and depends on the sphere size parameter $x_i = ka_i$ and the refractive index m_i , and the matrix H^{i-j} translates an outgoing VSH centered about origin j into an expansion of regular VSH centered about i . This translation matrix will be a function solely of the distance and direction between origins i and j , and the elements of H involve summations of the scalar harmonic $h_w(kr_{i-j}) P_w^0(\cos \theta_{i-j}) \exp(iv\phi_{i-j})$ for $w = |n-l|, \dots, n+l$.

The sphere-sphere T^{i-j} matrix describes the scattered field produced at sphere i due to an incident field at j . All the effects of multiple scattering on the coupling of the fields between j and i are embedded within the matrix. For equal-size spheres with equal truncation limits of $L_i = L_S$, Eq. (10) represents $2N_S L_S (L_S + 2)$ linear equations for each column vector of T^{i-j} . The set of scattering coefficients obtained from Eq. (9), for a given incident field, provides a complete picture of the electromagnetic field in both the near- and far-field regions. In particular, the cross sections and the polarimetric scattering pattern can be obtained directly from the scattering coefficients.

For the application at hand—which deals with the exchange of thermal radiation—it will be necessary to identify the orientation-averaged absorption cross sections of the spheres. This can be done most effectively by utilizing the T matrix relationships, as described in Refs. 2 and 9. The relevant formula is

$$\langle C_{\text{abs},i} \rangle = \frac{2\pi}{k^2} \sum_{\mu,\nu} \bar{b}_\mu^i \sum_{j=1}^{N_S} \sum_{l=1}^{L_j} \sum_{k=-l}^l \sum_{q=1}^2 T_{\mu\nu\nu'j'l'q'}^{i-j} (T_{\mu\nu\nu'}^{i-j'})^* \quad (11)$$

In the above and in what follows, Greek subscripts are shorthand for degree/order/mode, i.e., $\nu = (klq)$. The matrix J is referred to as the regular VSH (or plane wave) translation matrix; it has the same structure as H , except with basis functions involving the spherical Bessel functions $j_w(kr)$ as opposed to the Hankel functions $h_w(kr)$. Superscript $*$ denotes complex conjugate, and \bar{b} is a positive real-valued property solely of sphere i and is defined by

$$\bar{b}_{np}^i = -\text{Re} \left(\frac{1}{\bar{a}_{np}^i} + 1 \right) \quad (12)$$

2.2.2 Expansion of the Absorption Cross Section. The detailed transfer of radiant energy among the particles—which has been anticipated in Eq. (5)—should be embedded within the formula for $\langle C_{\text{abs},i} \rangle$. This structure is not obvious in the definition given in Eq. (11), and an alternative definition is needed to elucidate the interactive form of the absorption cross section. The derivation makes use of the symmetry and contraction properties of the translation matrices, details of which are found in Refs. 2 and 10. The application of these properties ultimately leads to the relation

$$\langle C_{\text{abs},i} \rangle = -\frac{2\pi}{k^2} \sum_{\mu} \bar{b}_\mu^i \left[\text{Re} T_{\mu\mu}^{i-i} + \sum_{\nu} \bar{b}_\nu^i |T_{\mu\nu}^{i-i}|^2 + \sum_{j=1}^{N_S} \sum_{\nu} \sum_{j \neq i} \bar{b}_\nu^j |T_{\mu\nu}^{i-j}|^2 \right] \quad (13)$$

We now submit that each of the terms appearing in this formula can be interpreted according to the exchange formula appearing in Eq. (5). When multiplied by $4\pi I_{b,\lambda}(T_i) d\lambda$, the sum of the first and second terms on the right represent the net emissive power from sphere i . The third term accounts for the absorption of the net emissive power from i by all the other spheres in the ensemble. Consequently, we have

$$C_{\text{emis},i} = -\frac{2\pi}{k^2} \sum_{\mu} \bar{b}_\mu^i \left[\text{Re} T_{\mu\mu}^{i-i} + \sum_{\nu} \bar{b}_\nu^i |T_{\mu\nu}^{i-i}|^2 \right] \quad (14)$$

$$C_{\text{emis},i-j} = \frac{2\pi}{k^2} \sum_{\mu} \bar{b}_\mu^i \sum_{\nu} \bar{b}_\nu^j |T_{\mu\nu}^{i-j}|^2 \quad (15)$$

We will demonstrate in the following section that the formula for the exchange cross section is consistent with that obtained from a direct modeling of the emission mechanism. For now we note that the formulas have the required properties that were originally postulated for the cross sections. Due to the symmetry properties of T^{i-j} , the exchange emission cross sections in Eq. (15) will automatically satisfy the reciprocity condition in Eq. (3). When a sphere is nonabsorbing—which corresponds to $\bar{b} = 0$ for the sphere—the exchange cross section to the sphere will be zero. For a single isolated sphere the self-interaction T matrix reduced to $T_{\mu\nu}^{i-i} \rightarrow \bar{a}_\mu^i \delta_{\mu\nu}$, and using

$$\bar{b}_\mu^i = -\frac{1}{|\bar{a}_\mu^i|^2} (\text{Re} \bar{a}_\mu^i + |\bar{a}_\mu^i|^2) \quad (16)$$

it follows that

$$\begin{aligned} C_{\text{emis},i}|_{N_S=1} &= \frac{2\pi}{k^2} \sum_{\mu} [-\text{Re} \bar{a}_\mu^i - |\bar{a}_\mu^i|^2] \\ &= \frac{2\pi}{k^2} \sum_{n=1}^{L_1} \sum_{p=1}^2 (2n+1) [-\text{Re} \bar{a}_{np}^i - |\bar{a}_{np}^i|^2] \\ &= C_{\text{ext},i} - C_{\text{sca},i} = C_{\text{abs},i} \end{aligned} \quad (17)$$

In other words, the emission cross section for an isolated sphere becomes identical to the absorption cross section for the sphere.

2.2.3 An Alternate Approach. The formula for the exchange cross section in Eq. (15) is not at all unexpected. Indeed, this formula could have been derived in a few lines solely from Eqs. (3), (9), and (11). The emission cross section in Eq. (14), on the other hand, is somewhat less intuitive. However, it would not be inappropriate to question the entire validity of the results because we have derived cross sections related to emission without dealing explicitly with the emission process. In this section, we will demonstrate—using a formulation that is realistic yet economical—that our derivation is consistent with an emission model.

We will begin with the exchange cross section in Eq. (15), which shows that the geometrical dependence on energy exchange is contained solely within $|T^{i-j}|^2$. We note again that the sphere-sphere T^{i-j} matrix describes the scattered field at j that results from the presence of the incident field at i . In a broader sense, the incident field at i could be generalized to include any form of external or internal excitation of the sphere, which results in an outgoing (i.e., scattered) wave from the sphere. The source of excitation will obviously have bearing on the overall “harmonic content” of the outgoing wave, yet the mechanism which carries

the energy of the wave to the surrounding spheres—and which is described by the T^{j-i} matrix—will be independent of the excitation source.

In this sense, we can separate the “source” and “transfer” mechanisms to predict the emissive power carried from sphere i to j . The latter will be a function entirely of T^{j-i} , whereas the former will depend only on the properties of the emitting sphere. We also note that the identification of the relevant source characteristics for the sphere need not begin with the fundamental Rytov formulation. This problem has already been solved, and the solution has demonstrated the equivalence between the emission and absorption cross sections of the sphere. We contend that this equivalence is sufficient to establish the necessary characteristics of thermal emission for our multiple sphere problem.

To demonstrate, we note that thermal emission by an isolated sphere can be modeled by a distribution of randomly oriented dipole point sources within the sphere. Each dipole radiates a field that is uncorrelated with all other dipoles. Because of the lack of correlation among the sources, interference among waves emitted from separate dipoles will have no net effect on the total power radiated from the sphere. Moreover, because of the random orientation, the net wave emitted will be unpolarized. It is therefore consistent to compute the net power of the field emitted from the entire distribution of dipoles by computing the power of the field produced by a single dipole and then averaging (i.e., integrating) the power over the volume of the sphere and the orientation of the dipole.

A single dipole, located at an arbitrary point \mathbf{r}_d inside the sphere, will produce an outgoing wave from its origin. By using the addition theorem (applied with a propagation constant corresponding to the particle material, i.e., $k \rightarrow mk$), the outgoing wave from the dipole can be transformed into an outgoing VSH expansion, centered about the sphere origin, that is convergent at the interior surface of the sphere. We will denote the VSH expansion coefficients of this wave as $d_{mnp}(\mathbf{r}_d)$.

Each internal wave component will generate an external, outgoing VSH wave component given by

$$a_{mnp} = \bar{d}_{np} d_{mnp}(\mathbf{r}_d) \quad (18)$$

where \bar{d}_{np} denote the “transmission” coefficients of the sphere; these quantities are typically encountered in the solution for scattering by a layered sphere [11]. The total power radiated from the sphere will be $4\pi C_{\text{emis}} J_{b,\lambda} d\lambda$, with C_{emis} determined from integration of the Poynting vector over the surface of the sphere for the fixed dipole location \mathbf{r}_d , followed by integration of the dipole over volume and orientation. This results in

$$C_{\text{emis}} = -\frac{2\pi}{k^2} \sum_{n,m,p} \langle |a_{mnp}|^2 \rangle = -\frac{2\pi}{k^2} \sum_{n,m,p} |\bar{d}_{np}|^2 \langle |d_{mnp}(\mathbf{r}_d)|^2 \rangle \quad (19)$$

in which $\langle \cdots \rangle$ denotes integration over volume and orientation. The minus sign is included to make the cross section positive since power leaving the sphere would naturally be negative per our sign convention. We now use the fact that the emission cross section must equal the absorption cross section of the sphere, given by

$$C_{\text{emis}} = \frac{2\pi}{k^2} \sum_{n,m,p} |\bar{d}_{np}|^2 \bar{b}_{np} \quad (20)$$

In addition, the emitted intensity from the isothermal sphere must be isotropic, and this implies that the first, second, and higher directional moments of the volume-averaged Poynting vector—which would represent the coefficients in a Legendre polynomial expansion of the emitted intensity—must be zero. From this we can conclude that the volume and orientation averaging process must result in an orthogonal operation, so that

$$\langle d_{mnp}(\mathbf{r}_d) a_{klq}^*(\mathbf{r}_d) \rangle = \left| \frac{\bar{d}_{np}}{\bar{d}_{np}} \right|^2 \bar{b}_{np} \delta_{nl} \delta_{mk} \delta_{pq} \quad (21)$$

The orthogonality property identified in Eq. (21) is not explicitly needed to match Eqs. (19) and (20), yet it will play a role in the subsequent analysis.

We can now extend these results to the interaction matrix description of the scattered field. Since $a^j = T^{j-i} p^i$ describes the scattered field at j produced by an external plane wave (regular VSH) excitation at i , then $a^j = T^{j-i} (\bar{d}/\bar{a}) d^i$ will generate the scattered field due to an internal outgoing VSH excitation within i . Referring to Eq. (11), the absorption cross section at j , due to the power emitted at i , would therefore be

$$\begin{aligned} C_{\text{emis},j-i} &= \frac{2\pi}{k^2} \sum_{\mu} \sum_{\nu, \nu'} \bar{b}_{\mu}^j T_{\mu\nu}^{j-i} \frac{\bar{d}_{\nu}^i}{\bar{a}_{\nu}^i} \left(T_{\mu\nu}^{j-i} \frac{\bar{d}_{\nu'}^i}{\bar{a}_{\nu'}^i} \right)^* \langle d_{\nu}^i(\mathbf{r}_d) (d_{\nu'}^i(\mathbf{r}_d))^* \rangle \\ &= \frac{2\pi}{k^2} \sum_{\mu} \sum_{\nu} \bar{b}_{\mu}^j |T_{\mu\nu}^{j-i}| \bar{b}_{\nu}^i \end{aligned} \quad (22)$$

which is precisely the result obtained in Eq. (15). Likewise, the formula for the emission cross section, in Eq. (14), can be obtained via the dipole model by the calculation of the net power leaving sphere i .

2.3 Evaluation and Properties of the Emission and Exchange Cross Sections

2.3.1 Convergence. Narayanaswamy et al. observed that the convergence, in harmonic order, of their series expression for the radiative conductance between a pair of spheres is highly dependent on the gap distance $kd_{1-2} = k|\mathbf{r}_{1-2}| - ka_1 - ka_2$ separating the spheres [7]. In the limit of zero gap (i.e., spheres in contact), the series does not converge. This behavior can be anticipated by examining the properties of the interaction T^{i-j} matrix. Considering the specific case of two identical spheres, the T^{1-2} matrix will be given by the Born expansion of Eq. (10),

$$T^{1-2} = \bar{a} H^{1-2} \bar{a} + \bar{a} H^{1-2} \bar{a} H^{2-1} \bar{a} H^{1-2} \bar{a} + \cdots \quad (23)$$

in which matrix multiplication is implied. The above equation can now be substituted into Eq. (15), and the ratio test can be applied to determine the series convergence in harmonic order n since all of the terms in the series will be positive. After lengthy manipulations, it turns out that the ratio of the $n+1$ and n terms scale, in the limit of $n \rightarrow \infty$, as $(2x_S/(2x_S + kd))^4$. In the limit of $d \rightarrow 0$, we conclude that the series for the exchange cross section will not converge.

There is a simple physical explanation for this behavior. Our model takes the spheres to be at uniform yet distinct temperature, and heat transfer—via any mechanism—between two bodies at different temperatures will become infinite as the distance between the bodies vanishes. Narayanaswamy et al. suggested that the dielectric function would need to become a function of the wave vector to accurately model the radiative exchange for vanishing gap thicknesses [7]. Alternatively, we would submit that the model would need to incorporate finite-rate conductive heat transfer within each of the spheres to maintain temperature continuity at the contact point between the spheres. It is also important to remark that the gap-sensitive convergence behavior of the emission cross sections does not cross over to the absorption cross section. That is, even though $C_{\text{emis},1}$ and $C_{\text{emis},1-2}$ will become unbounded as the spheres approach contact, their difference—which is the absorption cross section of sphere 1—will remain finite. Furthermore, the absorption cross section will typically converge within the order limit prescribed by the Lorenz–Mie criterion for the individual spheres.

2.3.2 Calculation for Small Gap Thickness. An implication of the previous section is that the algorithms and codes that were

designed to calculate the plane wave absorption properties of the spheres cannot be blindly applied to the calculation of the emission and exchange cross sections for conditions of $kd \ll 1$. In such regimes the number of harmonic orders required for the convergence of the emission and exchange cross sections will significantly exceed the usual Lorenz–Mie truncation limit for the spheres [7]. The evaluation of the terms in Eq. (10), for such conditions, will require the calculation of Bessel and Hankel functions for orders that are significantly greater than the magnitude of their arguments; algorithms that are not specifically designed for such tasks are likely to fail due to overflow/underflow and/or loss-of-precision errors. In addition, the solution of Eq. (10) obviously becomes more difficult as the number of orders increases.

A computational strategy which circumvents these difficulties can be identified for the two-sphere case. We define a new interaction matrix Q via

$$Q_{\mu\nu}^{i-j} = (\bar{b}_\mu^i)^{1/2} T_{\mu\nu}^{i-j} (\bar{b}_\nu^j)^{1/2} \quad (24)$$

so that the exchange cross section is

$$C_{\text{emis},i-j} = \frac{2\pi}{k^2} \sum_{\mu} \sum_{\nu} |Q_{\mu\nu}^{i-j}|^2 \quad (25)$$

For the two-sphere case, and assuming that both spheres are identical, an interaction equation for Q^{1-2} can be obtained by combining Eq. (10) for $(i,j)=(2,2)$ and $(1,2)$ and eliminating T^{2-2} to yield

$$Q_{\mu\nu}^{1-2} - \sum_{\mu',\nu'} G_{\mu\mu'}^{1-2} G_{\mu'\nu'}^{2-1} Q_{\nu'\nu}^{1-2} = G_{\mu\nu}^{1-2} \bar{a}_\nu \bar{b}_\nu \quad (26)$$

with

$$G_{\mu\nu}^{i-j} = \bar{a}_\mu (\bar{b}_\mu)^{1/2} H_{\mu\nu}^{i-j} (\bar{b}_\nu)^{-1/2} \quad (27)$$

When both n and l are much greater than the translation distance $2x_S + kd$, we apply the large-order asymptotic limit to the Bessel and Hankel functions in the expansion for the translation matrix. The only significant terms for this case are for $p=q=1$. We can also align the spheres along a common z axis, for which the azimuthal degrees will become decoupled, i.e., $m=k$. These conditions result in

$$\begin{aligned} G_{mn1ml}^{1-2} &\approx \tilde{G}_{mn1}^{1-2} \\ &= -(-1)^{m+n} \frac{(2n+1)(\epsilon-1)}{n(\epsilon+1)+1} \left(\frac{enl}{2\pi} \right)^{1/2} \left(2 + \frac{kd}{x_S} \right)^{-n-l-1} \\ &\quad \times \frac{(1+n+l)^{1+n+l}}{(2n+1)^{n+1/2} (2l+1)^{n+1/2}} \\ &\quad \times \frac{\Gamma(n+\frac{1}{2}) \Gamma(l+\frac{1}{2}) \Gamma(n+l+1)}{2\Gamma(n+l+\frac{3}{2})} \\ &\quad \times (\Gamma(n+m+1) \Gamma(n-m+1) \Gamma(l+m+1) \\ &\quad \times \Gamma(l-m+1))^{-1/2} \end{aligned} \quad (28)$$

with

$$\tilde{G}_{mn1}^{2-1} = (-1)^{n+l} \tilde{G}_{mn1}^{1-2} \quad (29)$$

and

$$\bar{a}_{n1} \bar{b}_{n1} \approx \tilde{s}_n = - \frac{i(2n+1)\epsilon''}{(\epsilon^* - 1)(1+n(1+\epsilon))} \quad (30)$$

where $\epsilon = m^2 = \epsilon' + i\epsilon''$ is the complex permittivity of the sphere and $e=2.71828$.

The procedure to calculate the emission cross sections is to first calculate $G_{mnp\ mlq}^{1-2}$ using the exact formulas up to an order n , $l = L_E$, and then use the approximate \tilde{G} and \tilde{s} formulas for higher orders. For a given order n , \tilde{G}_{mn1} will be a maximum for $n=l$ and

falls off rapidly in magnitude as $|n-l|$ increases; in this respect we found it necessary to include \tilde{G} values only for $|n-l| \leq 100$. Equation (26) was then solved via the Born expansion per Eq. (23), and the exchange cross section was obtained from Eq. (25). Each multiplication stage in the Born expansion was carried to a maximum order n that satisfied a set convergence criterion for Eq. (25). The random-orientation absorption cross section of the spheres are calculated via Eq. (11)—for which the typical order truncation of $n = L_S \sim x_S$ is employed—and the emission cross section is obtained from the sum of the exchange and absorption cross sections.

2.3.3 Two-Sphere Case: Limiting Behavior for Small Gap Thickness. We can use the Born approximation in Eq. (23) and the asymptotic formulas in Eqs. (28) and (30) to develop an approximate formula for the exchange cross section for a pair of spheres in the limit of vanishing gap thickness. Key assumptions are that (1) the terms of order $n \approx x_S$ contribute a relatively small fraction to the summations in Eq. (25), so that the large-order approximations can be applied to all terms, and (2) only the first term in the Born series is retained. This results in

$$C_{\text{emis},1-2}(kd \ll 1) \approx \frac{2\pi}{k^2} \sum_{n=1}^{\infty} \sum_{l=1}^{\infty} \sum_{m=-(n,l)}^{(n,l)} |\tilde{G}_{mn1}^{1-2} \tilde{s}_n|^2 \quad (31)$$

The sum over m can be exactly represented by the generalized hypergeometric functions, which can then be approximated in terms of gamma functions for large n, l . Stirling's formula can then be applied to the gamma functions, and we again take the limiting forms of the resulting formula for large n, l . The substitution of $s=n+l$ and $t=n-l$ is then used to eliminate n and l , and the summations over s and t are approximated by integrals. The resulting formula is

$$\begin{aligned} C_{\text{emis},1-2}(kd \ll 1) &\approx \frac{2\pi}{k^2} \left(\frac{\epsilon''}{(\epsilon' + 1)^2 + \epsilon'^2} \right)^2 \left(2 + \frac{d}{a} \right)^{-2} \\ &\quad \times \left(\ln \left(\frac{2+d/a}{2} \right) \right)^{-1} \end{aligned} \quad (32)$$

Taking the limit $kd \rightarrow 0$ yields the sought result of

$$C_{\text{emis},1-2}(kd \rightarrow 0) \approx \frac{\pi}{k^2} \left(\frac{\epsilon''}{(\epsilon' + 1)^2 + \epsilon'^2} \right)^2 \frac{a}{d} \quad (33)$$

The $1/d$ dependence in Eq. (33) shows that emissive exchange, in the vanishing gap limit, is analogous to conductive heat transfer. Indeed, Narayanaswamy et al. [7] defined a thermal emission conductance via $\kappa_{\text{emis}} = q_{\text{emis},i-j} d / (T_1 - T_2)$ in the limit of $T_1 \rightarrow T_2$, and our analysis would indicate that this conductance would approach a constant as the gap approached zero. This behavior is consistent with the results shown in Ref. [7].

2.3.4 Two-Sphere Case: Limiting Behavior for Large Gap Thickness. In principle, the exchange of thermal radiation between two spheres that are separated by a sufficiently large distance can be described by radiative transfer theory. In this case, a sufficiently large distance would correspond to the situation in which each sphere is in the far-field zone of the radiation emitted from its neighbor. In addition, widely spaced spheres would have approximately equal emission and absorption cross sections because field interactions among the spheres would not significantly perturb the sphere properties from their single-scattering values. The exchange cross section would then be approximated by

$$C_{\text{emis},i-j} = \langle C_{\text{abs},i} \rangle F_{i-j} \frac{\langle C_{\text{abs},j} \rangle}{\pi a_j^2} \quad (34)$$

in which F_{i-j} is the geometrical radiative configuration factor from sphere i to j . This quantity describes the fraction of emitted energy from sphere i that intercepts sphere j assuming a geometrical limit. The presence in the formula of the absorption/ geometrical cross section ratio of j —which defines the absorption

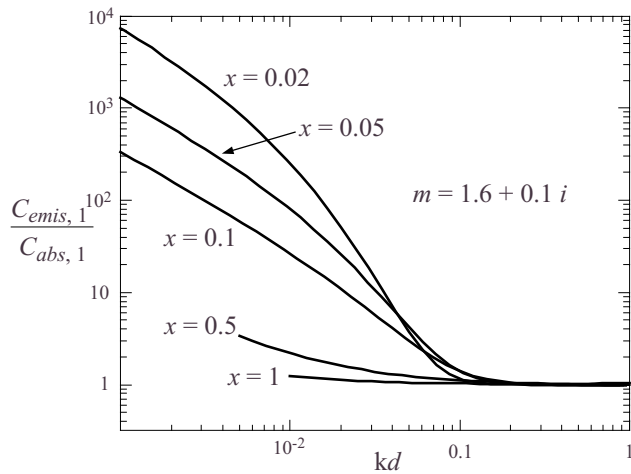


Fig. 2 Emission/absorption ratio for a sphere in a two-sphere cluster as a function of gap thickness kd

efficiency factor $\langle Q_{\text{abs},j} \rangle$ —represents an ad hoc correction to account for the effect of finite wavelength.

3 Results and Discussion

Although we have derived general formulas for the emission and exchange among an arbitrary number of closely spaced spheres, we will present and discuss results only for the case of two identical spheres. We do this to minimize the parameter space so that the effects of sphere spacing on emission and exchange can be better isolated and—perhaps more importantly—because we are currently incapable of accurately solving the emission and exchange problem for more than two spheres. We will also present spectral as opposed to wavelength-integrated results; doing so allows us to treat refractive index as a free parameter and obviates the need to characterize the refractive index of a specific material.

We focus first on the emission behavior as the sphere pair approaches contact. Shown in Fig. 2 is the ratio of the emission and absorption cross section, $C_{\text{emis},1}/\langle C_{\text{abs},1} \rangle$, for the two-sphere cluster as a function of dimensionless gap distance kd . Per our discussion in Sec. 2, the quantity $C_{\text{emis},1}/\langle C_{\text{abs},1} \rangle$ can be interpreted as the ratio of the total emission from sphere 1 to the emission transferred from 1 to the environment. The refractive index of the spheres is $m=1.6+0.1i$, and curves are shown for size parameters ranging from 0.02 to 1. Regardless of the size parameter, the emission/absorption ratio approaches unity once kd exceeds around 0.1. As kd decreases from 0.1, the emission/absorption ratio increases at a rate that is highly dependent on the size parameter. This effect is due almost entirely to an increase in the emission cross section; the absorption cross section, for the particular value of m , is not strongly dependent on the separation distance.

The behavior seen in Fig. 2 illustrates the effects of evanescent field coupling between the spheres. The fact that the onset of the coupling effects, for the different x values, occurs for the same value of kd would indicate that the thickness of the evanescent field layer is the same for all sphere size parameters at around $\sim 0.1/k$. Likewise, the amplified effects of coupling for the smaller spheres would also suggest a constant-thickness evanescent field layer; the smaller spheres will have a larger fraction of their surface coupled to the layer as the spheres become closer, and this would result in a larger relative increase in the emission cross section. We have performed additional calculations for spheres with a refractive index of $m=2+1i$ (not shown), and the behavior of $C_{\text{emis},1}/\langle C_{\text{abs},1} \rangle$ with kd is similar to that in Fig. 2 in that onset of near-field coupling occurs around $kd \sim 0.1$.

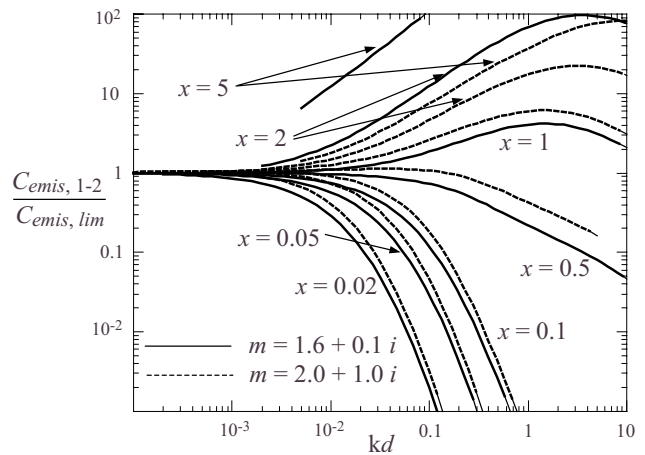


Fig. 3 Exchange cross section, scaled with a limiting value, as a function of gap thickness kd

The results in Fig. 2 indicate that the emission cross section approaches an inverse-linear relationship with kd as the gap approaches zero, which is consistent with our limiting-gap analysis. To examine this effect further, we show in Fig. 3 the exchange cross section scaled by the limiting form in Eq. (33) as a function of kd and with size and refractive index as parameters. For the particular refractive indices examined here, i.e., $m=1.6+0.1i$ and $2+1i$, the exchange cross sections for $x \leq 1$ asymptote to the limiting approximation in Eq. (33) as $kd \ll 1$. The results for larger size parameters appear to have the same trends, yet we were not able to obtain a converged solution, for these x values, for the sufficiently small kd values needed to check the limit.

We have also performed limited calculations of the emission and exchange cross sections for highly conducting materials, such as gold. The results for these materials appear to follow the same general trends shown in Fig. 3—in that the exchange cross section becomes inversely proportional to kd for $kd \ll 1$ —yet the conductivity value is somewhat different than that predicted in Eq. (33). That is, the curves in Fig. 3 for gold particles would asymptote to a constant other than unity. The inability of the limiting formula to accurately predict the behavior of metallic particles is likely a result of including only the first Born term in the approximation leading to Eq. (33). For the same reasons, we encountered significant numerical difficulties in finding converged solutions to Eq. (26) for metallic particles for small kd , and because of this we have put off the presentation of calculations for the metallic particles until we can resolve the numerical issues.

The last set of results will focus on the limiting behavior for $d/a \gg 1$, i.e., far-field exchange between the spheres. In Fig. 4 we plot $\pi a^2 C_{\text{emis},1-2} / C_{\text{abs},1}^2 (=Q_{\text{emis},1-2} / Q_{\text{abs},1}^2)$, where Q denotes the efficiency factors) versus d/a for the same parameters in Fig. 3. We choose this scaling because, based on our analysis leading to Eq. (34), the quantity should become a function solely of d/a for $kd \gg 1$. The results in the plot show, for the parameters examined here, that this is indeed the case. We include in Fig. 4 the geometrical-optics configuration factor (labeled GO) calculated for a pair of identical spheres using a simple Monte Carlo algorithm. Note that all curves asymptote to the geometrical formula once d/a exceeds around $1/x$ or, equivalently, $kd \gg 1$.

The curves for $x \leq 0.1$ in Fig. 4 display a transitional region around $d/a \sim 10$, which is between the evanescent field and far-field regions. As x becomes smaller, the slopes in this region (note that the plot is on a log-log scale) appear to approach the value of -5 , and the corresponding conductance between the spheres would have a dependence of d^{-6} in this region. It has been shown that the thermal emission conductance between two point dipoles scales as d^{-6} , and our results appear to be consistent with this

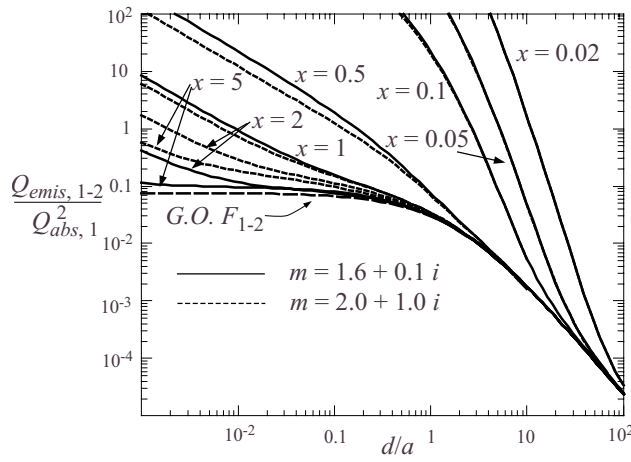


Fig. 4 Scaled exchange factor as a function of d/a

behavior for small x [7]. On the other hand, the results show that the region of the dipolelike behavior becomes increasingly small as the size parameters of the spheres increase.

4 Conclusions

We have presented an analysis of radiative emission and exchange among an ensemble of closely spaced, individually isothermal spheres. With regard to the theoretical framework of the problem, our analysis suggests that—for the case of neighboring spheres—the Rytov fluctuation-dissipation theory is not explicitly needed to identify the emission and exchange cross sections. Rather, these quantities can be deduced by the application of reciprocity and energy conservation principles to the solution to Maxwell's time harmonic wave equations for external (i.e., plane wave) excitation of the spheres. An asymptotic analysis of the exchange cross section indicates that the rate of emissive exchange between a pair of spheres becomes inversely proportional to d in the limit of $kd \rightarrow 0$.

Nomenclature

- a = sphere radius
- a_{mnp}^i = scattering expansion coefficient for sphere i
- \bar{a}_{np} = Lorenz–Mie coefficient
- \bar{b}_{np} = defined in Eq. (12)

- C = cross section
- d = gap distance between spheres, $=r_{1-2}-a_1-a_2$
- \mathbf{E} = electric field
- G^{i-j} = scaled H^{i-j} matrix, Eq. (27)
- H^{i-j} = outgoing VSH translation matrix
- J^{i-j} = regular VSH translation matrix
- $k = 2\pi/\lambda$
- m = refractive index, $=n+ik$
- Q = efficiency factor
- Q^{i-j} = scaled T^{i-j} matrix, Eq. (24)
- \mathbf{r} = position vector
- T_i = temperature of sphere i
- T^{i-j} = interaction T matrix for spheres i and j
- x_i = sphere size parameter, $=ka_i=2\pi a_i/\lambda$

Greek Symbols

- ϵ = permittivity, $=m^2=\epsilon'+i\epsilon''$
- λ = wavelength

References

- [1] Brunning, J. H., and Lo, Y. T., 1971, "Multiple Scattering of EM Waves by Spheres. Part I. Multipole Expansion and Ray-Optical Solutions," *IEEE Trans. Antennas Propag.*, **AP-19**, pp. 378–390.
- [2] Mackowski, D. W., and Mishchenko, M. I., 1996, "Calculation of the T Matrix and the Scattering Matrix for Ensembles of Spheres," *J. Opt. Soc. Am. A*, **13**, pp. 2266–2278.
- [3] Fuller, K. A., and Mackowski, D. W., 2000, "Electromagnetic Scattering by Compounded Spherical Particles," *Light Scattering by Nonspherical Particles: Theory, Measurements, and Applications*, M. I. Mishchenko, J. W. Hovenier, and L. D. Travis, eds, Academic, Chap. 8.
- [4] Kattawar, G. W., and Eisner, M., 1970, "Radiation From a Homogeneous Isothermal Sphere," *Appl. Opt.*, **9**, pp. 2685–2690.
- [5] Rytov, S. M., 1959, *Theory of Electric Fluctuations and Thermal Radiation*, Air Force Cambridge Research Center, Bedford, MA.
- [6] Mulet, J.-P., Joulain, K., Carminati, R., and Greffet, J.-J., 2001, "Nanoscale Radiative Heat Transfer Between a Small Particle and a Plane Surface," *Appl. Phys. Lett.*, **78**, pp. 2931–2933.
- [7] Narayanaswamy, A., Chen, D.-Z., and Chen, G., 2006, "Near-Field Radiative Energy Transfer Between Two Spheres," ASME Paper No. IMECE2006-15845.
- [8] Mishchenko, M. I., Travis, L. D., and Lacis, A. A., 2006, *Multiple Scattering of Light by Particles: Radiative Transfer and Coherent Backscattering*, Cambridge University Press, Cambridge, England.
- [9] Mackowski, D. W., 1994, "Calculation of Total Cross Sections of Multiple Sphere Clusters," *J. Opt. Soc. Am. A*, **11**, pp. 2851–2861.
- [10] Mackowski, D. W., 2001, "An Effective Medium Method for Calculation of the T Matrix of Aggregated Spheres," *J. Quant. Spectrosc. Radiat. Transf.*, **70**, pp. 441–464.
- [11] Bohren, C. F., and Huffman, D. R., 1983, *Absorption and Scattering of Light by Small Particles*, Wiley, New York.